Scientific Journals
An international open-access platform

Hanlin Letters

Article

OPEN ACCESS

Safety-Certified Robust Model Predictive Control for Managed Pressure Drilling Under Soluble Gas-Kick Transients

Nguyen Quang Huy,[1] Pham Duc Thinh[2]

[1] Hung Vuong University, 736 Nguyen Trai Street, Nong Trang Ward, Viet Tri, Phu Tho, Vietnam;
[2] Quy Nhon University, 170 An Duong Vuong Street, Nguyen Van Cu Ward, Quy Nhon, Binh Dinh, Vietnam;

Abstract
Deepwater and extended-reach drilling increasingly relies on managed pressure drilling to maintain bottomhole pressure within narrow operational windows while accommodating uncertain formation responses and complex annular hydraulics. Gas influx events remain difficult to handle because the observable surface signatures can be delayed or distorted by compressibility, slip, thermal gradients, and dissolution into non-aqueous drilling fluids. This paper develops a control-centric framework for gas-kick mitigation that treats the wellbore–riser system as a constrained dynamical plant and synthesizes a safety-certified robust model predictive controller for real-time choke and pump management. The core technical contribution is a compact, control-oriented thermo-solutal drift-flux model whose parameters are structured to support uncertainty sets and whose state representation explicitly tracks both free and dissolved gas inventories. The controller minimizes deviation from a pressure trajectory consistent with pore and fracture bounds while enforcing state and input constraints on wellhead pressure, choke actuation rate, circulating flow, and pit-volume growth. Robustness is addressed via tube-based tightening and stochastic disturbance models that capture sensor error, unmodeled friction, and uncertain mass transfer. Safety certification is provided by embedding control barrier constraints that guarantee forward invariance of a conservative safe set even when the predictive model is imperfect. Numerical studies across circulation regimes show that the proposed design can reduce peak pressure excursions and mitigate rapid riser unloading tendencies under plausible uncertainty magnitudes, while maintaining feasible control actions compatible with typical surface equipment limits. The framework is intended to unify mechanistic kick physics with modern constrained control in a manner suitable for automation and supervisory decision support.

1. Introduction

Managed pressure drilling (MPD) is increasingly deployed in environments where the allowable margin between pore pressure and fracture pressure is small, where operational transients are frequent, and where downhole conditions evolve rapidly with depth and temperature [1]. The MPD objective is often described as maintaining bottomhole pressure (BHP) inside a window, but in practice it is a multi-objective problem with coupled hydraulic, mechanical, and operational constraints. Circulation changes impose frictional transients that can threaten fracture integrity; choke adjustments can induce large surface pressure changes and propagate downhole with delays; and gas influx can grow from an initially subtle perturbation into a high-consequence event as the gas expands, accelerates, and potentially unloads the riser. The presence of synthetic- or oil-based drilling fluids adds an additional layer of complexity because methane or other hydrocarbon gases can dissolve into the liquid phase, altering the effective compressibility and delaying the appearance of free gas at the surface.

A significant technical challenge is that conventional well control procedures and many automation proposals implicitly assume that influx dynamics are adequately represented by free-gas models with simple slip closures and quasi-steady friction [2]. These assumptions may be adequate for certain water-based systems or for late-stage large kicks, but they can be misleading during early or moderate influx conditions where solubility and thermal effects alter the timing and shape of observables such as

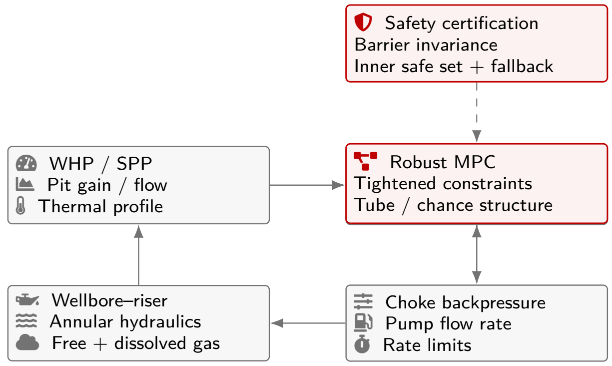

Figure 1: Closed-loop architecture for managed pressure drilling under soluble gas-kick transients. Surface measurements feed a state estimator that tracks pressure, thermal state, and both free and dissolved gas inventories. A robust MPC computes choke and pump actions under operational constraints, while a barrier-based safety layer enforces forward invariance of a conservative safe set and provides a certified fallback when tracking objectives conflict with safety.

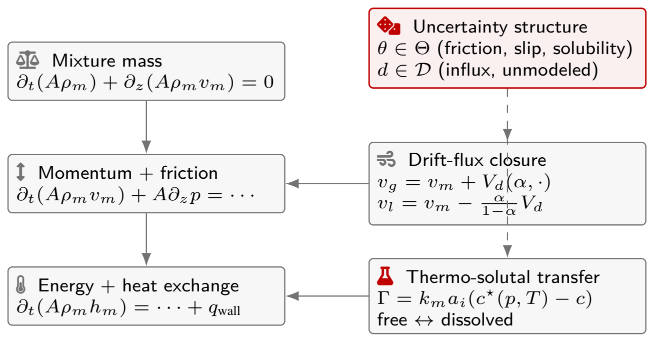

Figure 2: Control-oriented thermo-solutal drift-flux model decomposition. The dynamics combine mixture mass and momentum with a compact drift-flux slip closure, an energy balance for temperature-dependent density/solubility effects, and an explicit free/dissolved inventory exchange term. Key physical parameters and the influx disturbance are organized into structured sets to support robust prediction and constraint-aware control.

wellhead pressure and pit gain. A broad review of early gas-kick detection models emphasizes that the prevailing transient two-phase formulations are predominantly one-dimensional and often incorporate only limited heat transfer and solubility, while also noting that more sophisticated multiphase descriptions can improve the fidelity of phase velocity, temperature, and pressure fields relevant to operational response [3]. From a control standpoint, this observation motivates models that are richer than static correlations but still structured for real-time optimization and stability analysis, since MPD control must act continuously rather than merely diagnose.

This paper approaches kick mitigation as a constrained feedback control problem rather than as a pure simulation or detection problem. The central question is how to select surface actions, primarily choke pressure and pump rate, to keep the system within a safe operational envelope while the multiphase state evolves under uncertain influx and uncertain physical parameters. The proposed framework uses model predictive control (MPC) because MPC naturally handles multivariable dynamics, hard constraints, and objectives that trade off pressure regulation with actuator smoothness [4]. However, standard MPC can fail in safety-critical regimes if feasibility is lost or if model mismatch is large. The framework therefore couples robust MPC with explicit safety certification through control barrier constraints, providing a systematic method to maintain invariance of conservative safe sets even under uncertainty and transient multiphase behavior.

The technical contribution is organized around three requirements that are frequently in tension in MPD automation. The model must represent the essential physical mechanisms that shape pressure and gas migration, including solubility and thermal coupling, yet it must be compact enough for online optimization. The controller must enforce multiple operational constraints, including those that are naturally stated as inequalities on BHP, wellhead pressure, pit gain, and actuator limits, while also being

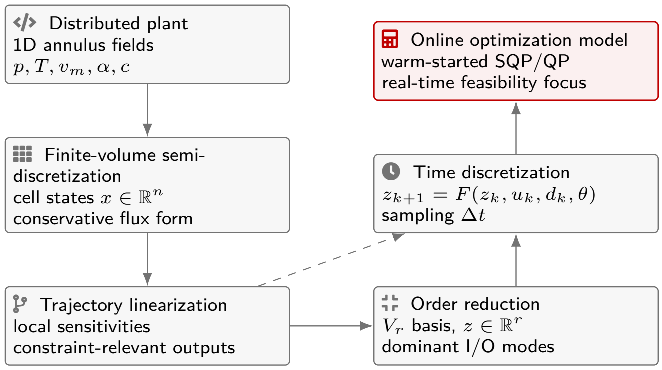

Figure 3: Prediction-model preparation pipeline for real-time control. The thermo-solutal PDE plant is discretized in conservative finite-volume form, linearized along an operating trajectory, and reduced to a compact state representation that preserves pressure and pit-gain dynamics. The reduced model is then discretized in time to provide a tractable predictive model for sequential quadratic optimization in robust MPC.

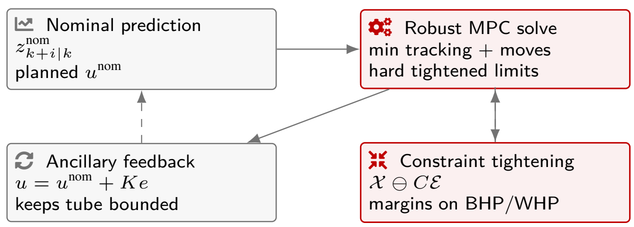

Figure 4: Tube-based robust MPC structure for kick mitigation. A nominal trajectory is optimized under tightened constraints that account for bounded disturbances and parameter uncertainty. A local ancillary feedback law confines the true trajectory to a bounded tube around the nominal prediction, enabling conservative satisfaction of bottomhole and wellhead pressure limits while keeping actuation changes feasible for surface equipment.

robust to uncertain friction, uncertain slip, and uncertain mass transfer [5]. Finally, the closed-loop behavior must be certifiable in the sense that the system remains within a defined safe region for all disturbances in an admissible set, not merely on average or in nominal scenarios.

The remainder of the paper develops these elements in a unified manner. A control-oriented thermo-solutal drift-flux model is introduced and discretized into a form suitable for MPC, with an uncertainty structure aligned with available engineering bounds. A robust MPC formulation is then derived, including constraint tightening that accounts for bounded disturbances and chance constraints that handle stochastic measurement and modeling errors. Safety certification is achieved by embedding barrier-based invariance conditions directly into the predictive optimization, yielding a controller that preserves feasibility and safety margins under conservative assumptions [6]. Numerical studies illustrate the interaction between dissolution, circulation, and choke actions, highlighting regimes where solubility can shift the optimal response and where safety certification prevents aggressive but risky actions.

2. Control-Oriented Thermo-Solutal Drift-Flux Model

The plant considered is a coupled wellbore–riser annulus in which a drilling fluid circulates and where a gas influx may occur at a downhole location. The modeling goal is not to reproduce all multiphase flow regimes with maximal fidelity, but to capture the mechanisms that drive constraint-relevant variables in MPD control, particularly BHP, wellhead pressure, surface return flow, and pit-volume evolution. The model is therefore one-dimensional in measured depth, includes compressibility, slip, and heat transfer in a simplified form, and represents gas dissolution and exsolution through a thermodynamically constrained inventory model [7]. This choice supports online optimization while preserving the dominant nonlinearities that shape the response to choke and pump actions.

Let $z \in [0, L]$ denote the axial coordinate with $z = 0$ at the wellhead and $z = L$ at the bottom boundary of the modeled domain. The annular cross-sectional area is $A(z)$, the hydraulic diameter is $D_h(z)$, and the inclination

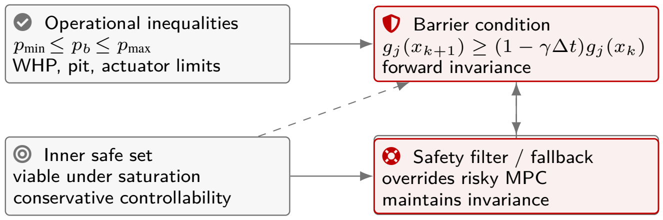

Figure 5: Safety certification embedded in predictive control via barrier constraints. Operational limits define a safe set, while discrete-time barrier inequalities constrain control actions so safety margins cannot collapse too rapidly between sampling instants. Robustification accounts for admissible disturbances and parameter uncertainty, and an inner viable set plus safety filter provides a certified fallback when tracking objectives threaten invariance.

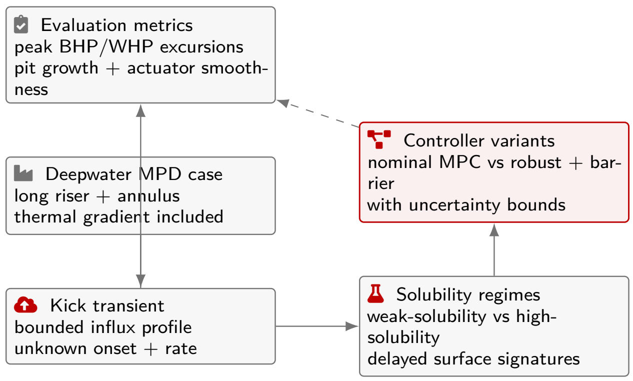

Figure 6: Numerical study blueprint used to stress the controller under soluble gas-kick transients. A representative deepwater MPD configuration is excited by a bounded influx disturbance and evaluated across weak- and high-solubility assumptions to expose delayed observables and near-surface release tendencies. Performance is assessed through pressure constraint adherence, pit-volume behavior, and actuator feasibility under uncertainty-aware predictive control and barrier certification.

is $\theta(z)$. The mixture consists of a liquid drilling fluid and a gas phase that may be present as free gas with volume fraction $\alpha(z,t)$ and as dissolved gas with concentration $c(z,t)$ defined per unit mass of liquid. The primary field variables are pressure $p(z,t)$, mixture superficial velocity $v_m(z,t)$, temperature $T(z,t)$, free-gas holdup $\alpha(z,t)$, and dissolved concentration $c(z,t)$ [8].

A conservative finite-volume formulation begins with mixture mass conservation,

$$\frac{\partial}{\partial t}(A\rho_m) + \frac{\partial}{\partial z}(A\rho_m v_m) = 0, \tag{1}$$

where $\rho_m = \alpha\rho_g + (1-\alpha)\rho_l$ is the mixture density, $\rho_g = \rho_g(p,T)$ is gas density, and $\rho_l = \rho_l(p,T,c)$ is liquid density allowing weak dependence on dissolved gas through swelling. Gas mass is partitioned into free and dissolved inventories. The free-gas mass balance is

$$\frac{\partial}{\partial t}(A\alpha\rho_g) + \frac{\partial}{\partial z}(A\alpha\rho_g v_g) = -A\Gamma + A s_g, \tag{2}$$

and the dissolved-gas balance is [9]

$$\frac{\partial}{\partial t}(A(1-\alpha)\rho_l c) + \frac{\partial}{\partial z}(A(1-\alpha)\rho_l c\, v_l) = A\Gamma, \tag{3}$$

where $\Gamma(z,t)$ is the interphase mass-transfer rate (positive for dissolution, negative for exsolution) and s_g is a distributed source term that is typically zero except at an influx boundary. Phase velocities are linked to mixture velocity through a drift-flux closure,

$$v_g = v_m + V_d(\alpha,p,T;\eta), \quad v_l = v_m - \frac{\alpha}{1-\alpha} V_d(\alpha,p,T;\eta), \tag{4}$$

with V_d a drift velocity parameterized by a small set η that captures buoyancy and annular geometry effects in a differentiable manner. The closure must be flexible enough to represent changes between circulating and non-circulating conditions because circulation alters slip by modifying turbulence and by advecting bubbles.

Symbol	Description	Dependence
$p(z,t)$	Pressure	z,t
$T(z,t)$	Temperature	z,t
$v_m(z,t)$	Mixture superficial velocity	z,t
$\alpha(z,t)$	Free-gas volume fraction	z,t
$c(z,t)$	Dissolved-gas concentration (per unit liquid mass)	z,t
$\rho_m(z,t)$	Mixture density	z,t

Table 1: Distributed state variables used in the control-oriented thermo-solutal drift-flux model.

Symbol	Description	Appears in
$\alpha\rho_g$	Free-gas mass per unit mixture volume	Free-gas mass balance
$(1-\alpha)\rho_l c$	Dissolved-gas mass per unit mixture volume	Dissolved-gas balance
$c^\star(p,T;\chi)$	Equilibrium dissolved-gas concentration	Solubility relation in Γ
$\Gamma(z,t)$	Interphase mass-transfer rate (dissolution/exsolution)	Gas inventory coupling
$\dot{m}_{\text{in}}(t)$	Gas influx mass-flow disturbance at depth	Bottom boundary condition

Table 2: Gas inventories and mass-transfer quantities linking free and dissolved phases.

Momentum is represented at the mixture level with friction and gravity, [10]

$$\frac{\partial}{\partial t}(A\rho_m v_m) + \frac{\partial}{\partial z}(A\rho_m v_m^2) + A\frac{\partial p}{\partial z} = -A\rho_m g\cos\theta - A\Delta_w. \quad (5)$$

where Δ_w is the wall shear contribution expressed per unit volume. For control purposes, Δ_w is modeled with an effective friction factor f_{eff} and mixture viscosity μ_{eff},

$$\Delta_w = \frac{2f_{\text{eff}}(\text{Re}_m,\alpha;\xi)\rho_m v_m|v_m|}{D_h}, \qquad \text{Re}_m = \frac{\rho_m|v_m|D_h}{\mu_{\text{eff}}(\alpha,T;\xi)}, \quad (6)$$

where ξ collects uncertain friction and rheology parameters. In practice, drilling fluids are often non-Newtonian and can be modeled by Herschel–Bulkley or similar laws, but for MPC it is often sufficient to use a smooth surrogate whose parameters can be bounded and updated offline. The crucial requirement is that friction uncertainty be represented explicitly because it directly affects the mapping from surface actions to BHP and thus affects constraint satisfaction [11].

Thermal coupling is included through a simplified energy equation in mixture form,

$$\frac{\partial}{\partial t}(A\rho_m h_m) + \frac{\partial}{\partial z}(A\rho_m v_m h_m) = -Av_m\frac{\partial p}{\partial z} + Aq_{\text{wall}}(T,T_f;\kappa). \quad (7)$$

where h_m is mixture specific enthalpy, $T_f(z)$ is an ambient formation or seawater temperature profile, and q_{wall} models heat exchange with coefficient κ. The energy equation influences solubility and compressibility through the dependence of ρ_g and equilibrium dissolution on temperature. From a control perspective, including T helps prevent the controller from attributing temperature-driven density changes to influx, which could otherwise cause inappropriate choke actions.

Solubility is represented through a constrained equilibrium concentration $c^\star(p,T;\chi)$ and a finite-rate mass-transfer law,

$$\Gamma = k_m a_i(c^\star(p,T;\chi) - c), \qquad a_i = \frac{6\alpha}{d_b(\alpha,p,T;\nu)}, \quad (8)$$

where k_m is a mass-transfer coefficient, a_i is interfacial area density, and d_b is an effective bubble diameter parameterized by ν [12]. The equilibrium map $c^\star$ encapsulates the pressure- and temperature-dependent solubility capacity of the drilling fluid, which can be substantially larger in synthetic- or oil-based systems than in water-based systems. The parameters χ represent effective solubility behavior and are treated as uncertain within bounds derived from laboratory PVT measurements or conservative engineering estimates. This modeling choice is aligned with practical control needs because it allows the controller to anticipate that a portion of influx mass can remain dissolved at depth and later exsolve as pressure decreases, producing delayed free gas and potentially rapid unloading near the surface.

Quantity	Symbol	Role	Uncertainty
Drift velocity	$V_d(\alpha, p, T; \eta)$	Slip between phases	Parameters η
Hydraulic diameter	$D_h(z)$	Geometric scale for friction	Known well/riser profile
Effective friction factor	$f_{\text{eff}}(\text{Re}_m, \alpha; \xi)$	Wall shear closure	Parameters ξ
Mixture viscosity	$\mu_{\text{eff}}(\alpha, T; \xi)$	Defines Re_m	Rheology surrogate
Mixture Reynolds number	Re_m	Flow-regime indicator	Derived from v_m, ρ_m
Wall shear term	Δ_w	Momentum sink in annulus	Built from f_{eff}

Table 3: Hydraulic and drift-flux quantities governing slip and frictional pressure losses.

Symbol	Description	Affects	Calibration source
h_m	Mixture specific enthalpy	Energy storage and transport	Fluid thermodynamics
$q_{\text{wall}}(T, T_f; \kappa)$	Heat flux with formation/seawater	Temperature profile	Thermal characterisation
$T_f(z)$	Ambient formation or seawater temperature	Solubility and density	Geothermal / riser profile
k_m	Mass-transfer coefficient	Rate of Γ	Lab PVT / mass-transfer data
a_i	Interfacial area density	Magnitude of Γ	Bubble size correlations
$d_b(\alpha, p, T; \nu)$	Effective bubble diameter	a_i and slip behavior	Tuning parameter ν
$c^\star(p, T; \chi)$	Equilibrium solubility map	Dissolved inventory	Solubility measurements

Table 4: Thermal and solubility-related quantities in the thermo-solutal model.

The literature contains semi-analytical and mechanistic kick models that explicitly account for these solubility effects and for the distinct behavior of annular flow compared with pipe correlations, and such works have been presented as state-of-the-art treatments of gas kick modeling and methane dissolution in synthetic or oil-based drilling fluids [13]. Complementary mechanistic modeling focused on riser dynamics and analytic solubility prediction for methane in synthetic-based mud has also been presented, including comparisons against process simulation and experimental observations, which further shows the operational relevance of dissolution in deepwater kick scenarios [14]. The present work uses these observations as motivation to include dissolution explicitly in a control-oriented state representation, without centering the control design around any particular prior simulator.

Boundary conditions connect the distributed plant to surface actuators [15]. The primary control inputs are choke backpressure at the wellhead and pump flow rate, denoted $u(t) = [p_c(t), Q_p(t)]^\top$, where p_c is the pressure imposed by the choke manifold and Q_p is circulation flow rate. The surface pressure boundary can be written as

$$p(0, t) = p_c(t) + p_{\text{sep}}(t), \tag{9}$$

where p_{sep} is separator or downstream pressure treated as measured or slowly varying. The pump sets an inflow boundary for mixture mass flux, with the mapping from Q_p to downhole v_m depending on fluid density and geometry. The influx is treated as a disturbance or an uncertain input at the bottom boundary, entering as a gas mass flux $\dot{m}_{\text{in}}(t)$ and possibly a liquid flux if formation fluids other than gas are considered. For the purpose of kick mitigation, the primary uncertainty is the gas influx rate and its time variation; this disturbance drives constraint violations if uncontrolled.

For MPC, the PDE model is discretized into a finite-dimensional state-space system. Let $x(t) \in \mathbb{R}^n$ collect cell-averaged values of p, T, v_m, α, c across the mesh. The semi-discrete dynamics can be written as [16]

$$\dot{x}(t) = f(x(t), u(t), d(t), \theta), \quad y(t) = h(x(t), u(t), \theta) + w(t), \tag{10}$$

where $d(t)$ is the disturbance vector including influx and unmodeled transients, θ collects uncertain physical parameters, $y(t)$ are measured outputs including wellhead pressure, standpipe pressure, and pit volume, and $w(t)$ is measurement noise. Because n can be large, a reduced-order representation is often desirable. For control, a projection-based reduction can be formed by linearizing about an operating trajectory and applying balanced truncation or energy-weighted proper orthogonal decomposition, yielding

$$x(t) \approx x_0(t) + V_r z(t), \quad \dot{z}(t) = f_r(z(t), u(t), d(t), \theta), \tag{11}$$

where $z(t) \in \mathbb{R}^r$ with $r \ll n$ and V_r is a basis that preserves the dominant input–output dynamics relevant to pressure and pit gain. Reduction is performed with care

Quantity	Symbol	Measurement location	Use in control
Bottomhole pressure	$p_b(t)$	Near $z = L$ (or extrapolated)	Primary pore/fracture constraint
Wellhead pressure	$p_w(t) = p(0,t)$	Surface annulus	Surface and riser protection
Pit volume	$V_p(t)$	Active mud system	Influx indicator and volume limit
Choke pressure	$p_c(t)$	Choke manifold	Manipulated backpressure input
Pump flow rate	$Q_p(t)$	Standpipe/pump	Manipulated circulation input
Standpipe pressure	$p_{\text{sp}}(t)$	Drillstring	State estimation and monitoring

Table 5: Measured outputs and manipulated variables used in the MPD control loop.

Constraint	Lower bound	Upper bound	Interpretation
Bottomhole pressure window	$p_{\min}(t)$	$p_{\max}(t)$	Pore and fracture limits
Wellhead pressure	$p_{w,\min}$	$p_{w,\max}$	Riser and surface equipment limits
Choke pressure	$p_{c,\min}$	$p_{c,\max}$	Choke manifold operating range
Choke rate of change	$-r_c$	r_c	Actuator slew limitation
Pump flow rate	0	$Q_{\max}$	Pump capacity constraint
Pump rate of change	$-r_p$	r_p	Pump ramp limitation
Pit-volume growth	0	$\dot{V}_{p,\max}$	Surface-handling constraint

Table 6: Operational inequality constraints represented in the MPC formulation.

to preserve constraint-relevant outputs, particularly BHP and wellhead pressure, because MPC feasibility depends on accurate output prediction [17]. The reduced model is then discretized in time with sampling period Δt to form a prediction model for MPC,

$$z_{k+1} = F(z_k, u_k, d_k, \theta), \quad y_k = H(z_k, u_k, \theta), \tag{12}$$

where k indexes control intervals.

3. Robust MPC Formulation for MPD Kick Mitigation

The control objective is to keep the system within operational safety constraints while minimizing deviations from desired pressure behavior and limiting aggressive actuator movement. MPD constraints are naturally expressed as inequalities on BHP and on fracture margins, as well as on surface equipment limitations. Let $p_b(t)$ denote bottomhole pressure, which is typically approximated as $p(L,t)$ plus a correction term if the modeled domain does not include the full depth [18]. Let $p_w(t) = p(0,t)$ denote wellhead pressure. Let $V_p(t)$ denote pit volume, whose rate of change depends on the imbalance between pumped inflow and returned outflow and is influenced by compressibility and gas expansion. The controller must enforce constraints of the form

$$p_{\min}(t) \le p_b(t) \le p_{\max}(t), \quad p_{w,\min} \le p_w(t) \le p_{w,\max}, \tag{13}$$

where $p_{\min}$ corresponds to pore-pressure-based lower bounds and $p_{\max}$ corresponds to fracture or casing shoe limits. Additional constraints include choke pressure bounds and rate limits,

$$p_{c,\min} \le p_c(t) \le p_{c,\max}, \quad |\dot{p}_c(t)| \le r_c, \tag{14}$$

and pump constraints, [19]

$$0 \le Q_p(t) \le Q_{\max}, \quad |\dot{Q}_p(t)| \le r_p. \tag{15}$$

Pit-volume growth is constrained to limit surface handling risk,

$$V_p(t) \le V_{p,\max}, \quad \dot{V}_p(t) \le \dot{V}_{p,\max}, \tag{16}$$

with the understanding that V_p measurements can be noisy and filtered, and that constraint enforcement may require a conservative margin.

In MPC, these constraints are enforced over a prediction horizon N. Using the reduced-order discrete-time model, the nominal MPC problem at time step k selects a control sequence $\mathbf{u}_k = \{u_{k|k}, u_{k+1|k}, \ldots, u_{k+N-1|k}\}$

Cost term	Weight	Physical meaning	Effect on control action
$\|p_b - p_{b,\text{ref}}\|^2$	Q_b	BHP tracking	Centers BHP in operational window
$\|p_w - p_{w,\text{ref}}\|^2$	Q_w	Wellhead pressure tracking	Limits surface pressure excursions
$\|u_k - u_{k-1}\|^2$	R	Move suppression	Smooths choke and pump adjustments
$\|u_k - u_{\text{ref}}\|^2$	S	Deviation from preferred operating point	Keeps operation near nominal settings

Table 7: Structure of the stage cost used in the robust MPC objective.

Quantity	Symbol	Uncertainty set	Main source
Gas influx rate	$\dot{m}_{\text{in}}(t)$	$\mathcal{D}_{\text{in}}$	Unknown formation inflow profile
Friction/rheology parameters	ξ	Ξ	Non-Newtonian fluid behaviour
Drift-flux parameters	η	$\mathcal{H}$	Slip and holdup correlations
Solubility-map parameters	χ	$\mathcal{X}$	PVT and solubility data scatter
Mass-transfer coefficient	k_m	$\mathcal{K}$	Interfacial transport uncertainty
Measurement noise	w_k	$\mathcal{W}$	Sensor and filtering errors

Table 8: Uncertainty sets entering the robust MPC and safety-certification design.

to minimize a cost function subject to predicted dynamics and constraints. A representative cost is

$$J_k(\mathbf{u}_k) = \sum_{i=0}^{N-1} \Big(\|p_{b,k+i|k} - p_{b,\text{ref},k+i}\|^2_{Q_b} + \|p_{w,k+i|k} - p_{w,\text{ref},k+i}\|^2_{Q_w} + \|u_{k+i|k} - u_{k+i-1|k}\|^2_R + \|u_{k+i|k} - u_{\text{ref},k+i}\|^2_S \Big), \tag{17}$$

where Q_b, Q_w, R, S are weighting matrices, $p_{b,\text{ref}}$ and $p_{w,\text{ref}}$ are reference trajectories consistent with a desired equivalent circulating density, and u_{ref} encodes preferred operating points such as nominal choke pressure and nominal pump rate. The inclusion of both tracking and move suppression reflects the operational preference for smooth actuation to reduce wear and avoid inducing additional transients [20].

Nominal MPC can be inadequate because the influx rate and physical parameters are uncertain. Robust MPC addresses this by ensuring constraint satisfaction for all disturbances within an admissible set. Let d_k represent disturbances, including influx rate uncertainty and unmodeled friction, bounded by $d_k \in \mathcal{D}$, and let parameter uncertainty be represented as $\theta \in \Theta$ where Θ is a compact set constructed from engineering bounds. A conservative robust MPC formulation seeks controls such that constraints hold for all $(d, \theta) \in \mathcal{D} \times \Theta$, but this can be computationally demanding for nonlinear multiphase models. The proposed framework uses a tube-based approach: a nominal prediction is optimized, and an ancillary feedback law keeps the true trajectory within a bounded tube around the nominal trajectory, allowing constraints to be tightened on the nominal system.

Let z_k be the reduced state and z_k^{nom} be the nominal predicted state. Define the error $e_k = z_k - z_k^{\text{nom}}$. Under a stabilizing local feedback $u_k = u_k^{\text{nom}} + Ke_k$, the error dynamics can be bounded under Lipschitz assumptions on the nonlinear model. The tube set $\mathcal{E}$ is chosen such that if $e_k \in \mathcal{E}$ then $e_{k+1} \in \mathcal{E}$ for all admissible disturbances. Constraint tightening then replaces the original constraint set $\mathcal{X}$ with a tightened set $\mathcal{X} \ominus C\mathcal{E}$ where C maps state error to constraint-relevant outputs. In output form, the tightened BHP and wellhead constraints become [21]

$$\begin{aligned} p_{\text{min}}(k) + \delta_b \le p^{\text{nom}}_{b,k|k} \le p_{\text{max}}(k) - \delta_b, \\ p_{w,\text{min}} + \delta_w \le p^{\text{nom}}_{w,k|k} \le p_{w,\text{max}} - \delta_w, \end{aligned} \tag{18}$$

where δ_b, δ_w are margins computed from worst-case output deviations induced by $e_k \in \mathcal{E}$. These margins can be updated online if the uncertainty bounds change, for example when the drilling fluid rheology is updated or when temperature gradients evolve.

While tube MPC handles bounded disturbances, some uncertainties are better represented probabilistically, particularly measurement noise and small unmodeled fluctuations. A chance-constrained extension replaces hard constraints with probabilistic ones, such as

$$\begin{aligned} \mathbb{P}(p_{\text{min}}(k) \le p_b(k) \le p_{\text{max}}(k)) \ge 1 - \epsilon_b, \\ \mathbb{P}(p_{w,\text{min}} \le p_w(k) \le p_{w,\text{max}}) \ge 1 - \epsilon_w, \end{aligned} \tag{19}$$

with violation probabilities ϵ_b, ϵ_w selected according to operational risk tolerance. In practice, these constraints can be approximated by tightening based on variance es-

Scenario	Mud system	Circulation regime	Key feature studied
S1	Weak-solubility (water-based)	Steady circulation	Prompt free-gas signatures and basic response
S2	High-solubility (synthetic-based)	Steady circulation	Delayed surface indicators due to dissolution
S3	High-solubility (synthetic-based)	Reduced / no circulation	Migration and expansion under low flow
S4	High-solubility with uncertainty	Mixed circulation changes	Conservatism and viability under large bounds

Table 9: Representative numerical scenarios used to illustrate closed-loop behaviour.

timates from an extended Kalman filter or ensemble predictor [22]. The advantage is that the controller can avoid excessive conservatism when uncertainty is dominated by small stochastic variations rather than large bounded disturbances. The framework can blend bounded and stochastic representations by treating influx as bounded but unknown and treating sensor noise as Gaussian, yielding a mixed robust–stochastic tightening.

A distinctive aspect of MPD under soluble gas kicks is that dissolution can reduce immediate free-gas holdup while storing gas mass in the liquid, and subsequent exsolution can create rapid near-surface gas release. This alters the effective disturbance dynamics. From a control perspective, it means the disturbance is not simply an additive term; it changes the state evolution through coupled inventory dynamics [23]. The robust MPC formulation therefore treats solubility and mass transfer parameters as uncertain, not merely the influx rate. The set Θ includes bounds on χ and k_m, and the tube margins are computed under these bounds. This approach is conservative but consistent with safety requirements because uncertainty in solubility capacity can meaningfully affect the timing of gas appearance and thus the required choke response.

The MPC optimization is nonlinear due to the multiphase prediction model. To maintain real-time tractability, the framework employs a sequential quadratic programming (SQP) strategy with warm starts [24]. At each control interval, the model is linearized along the current nominal trajectory, and a quadratic approximation of the cost is formed. Constraints are linearized and tightened. The resulting quadratic program is solved to update the control sequence, and the first control action is applied. Because the plant is nonlinear and can exhibit stiffness during rapid gas expansion, the linearization must be handled carefully [25]. The reduced-order model is chosen to preserve the dominant nonlinearities in pressure response, and trust-region mechanisms limit step sizes to avoid divergence.

Feasibility is a central concern in safety-critical MPC. If constraints are too tight or if the model mismatch is large, the optimization may become infeasible, leading to undefined actions. The proposed framework integrates explicit safety certification, described next, to ensure that even when the MPC objective cannot be met, the controller defaults to actions that preserve invariance of a conservative safe set rather than violating constraints.

4. Safety Certification via Barrier-Constrained Predictive Control

Safety certification in this context means that the closed-loop system remains within a predefined safe set despite bounded uncertainty [26]. In MPD, the safe set is naturally defined by inequalities on BHP, wellhead pressure, choke limits, and pit volume. However, directly enforcing these constraints in MPC does not guarantee invariance because prediction errors and disturbances can cause the true state to exit the set between control updates or despite nominal satisfaction. Control barrier functions (CBFs) provide a mechanism for enforcing forward invariance by constraining the control input to ensure that a barrier function does not decrease too quickly. The challenge in multiphase MPD is to apply barrier logic to a reduced-order model while accounting for uncertainty and discretization.

Let the safe set be defined as [27]

$$\mathcal{S} = \{x : g_j(x) \geq 0 \text{ for all } j\}, \tag{20}$$

where each $g_j(x)$ corresponds to a safety margin, such as $g_b(x) = p_b(x) - p_{\text{min}}$ and $g_f(x) = p_{\text{max}} - p_b(x)$, along with similar functions for wellhead pressure and pit volume. In continuous time, a CBF condition for a relative-degree-one constraint is often expressed as

$$\dot{g}_j(x) + \gamma_j g_j(x) \geq 0, \tag{21}$$

with $\gamma_j > 0$ determining how aggressively the constraint is enforced near the boundary. In discrete time with sampling interval Δt, a compatible condition is

$$g_j(x_{k+1}) \geq (1 - \gamma_j \Delta t)\, g_j(x_k), \tag{22}$$

which ensures that if $g_j(x_k) \geq 0$ and the condition holds, then $g_j(x_{k+1}) \geq 0$ under suitable bounds. The condition becomes a constraint on the control input through the dynamics $x_{k+1} = f_d(x_k, u_k, d_k, \theta)$.

In a nonlinear uncertain system, ensuring the barrier condition for all disturbances is difficult. The framework adopts a robust barrier constraint by enforcing [28]

$$\min_{d_k \in \mathcal{D},\, \theta \in \Theta} g_j(f_d(x_k, u_k, d_k, \theta)) \geq (1 - \gamma_j \Delta t)\, g_j(x_k), \tag{23}$$

which guarantees invariance for all admissible uncertainties. This min condition can be conservative, but it aligns with safety requirements. In practice, it is approximated using a worst-case linearization or by sampling extreme points of $\mathcal{D} \times \Theta$ and enforcing the barrier constraint for each sample. Because the uncertainty sets are structured with small dimension, such sampling can be tractable. Alternatively, one can compute a conservative bound on the effect of uncertainty on g_j using Lipschitz constants, yielding a tightened deterministic constraint [29].

The barrier constraints are integrated into MPC by adding them as hard constraints at each predicted step. For the reduced state z_k and nominal control u_k^{nom}, the barrier constraint is applied to the nominal prediction with additional tightening to account for tube error. Denote the nominal next state as $z_{k+1}^{\text{nom}} = F(z_k^{\text{nom}}, u_k^{\text{nom}}, 0, \hat{\theta})$ where $\hat{\theta}$ is a nominal parameter, and let the worst-case deviation in the barrier function due to uncertainty and tube error be bounded by Δg_j. Then a sufficient condition for robust invariance is

$$g_j\left(z_{k+1}^{\text{nom}}\right) - \Delta g_j \geq (1 - \gamma_j \Delta t)(g_j(z_k^{\text{nom}}) - \Delta g_j), \tag{24}$$

which is conservative but provides a clear mechanism for certification. The quantities Δg_j can be computed online from current uncertainty bounds and local sensitivity estimates of g_j with respect to state and parameters. Because the model includes dissolution and thermal coupling, the sensitivity of BHP to choke pressure can vary with gas holdup and dissolved inventory; barrier constraints adapt to this variation by using local sensitivities rather than fixed gains [30].

A key advantage of barrier-constrained MPC is graceful degradation. When the nominal MPC objective is incompatible with safety constraints, the optimization prioritizes feasibility of barrier constraints, effectively overriding tracking objectives. This is particularly relevant during rapid gas expansion near the surface where aggressive choke opening might reduce wellhead pressure but could also induce a sudden reduction in BHP that violates pore pressure constraints. Barrier logic ensures that the controller does not sacrifice BHP safety for surface pressure comfort unless a controlled trade-off is explicitly permitted by redefining the safe set.

The integration of barrier constraints with robust MPC requires attention to feasibility [31]. If the safe set is too restrictive or if actuator limits prevent satisfying the barrier inequalities, infeasibility can still occur. The framework addresses this by defining a conservative inner safe set that is known to be controllable under worst-case conditions, and by using a fallback policy that maintains invariance within this inner set. The inner set can be computed offline by solving a viability problem on a reduced model, yielding state-dependent bounds on allowable pressures. In operation, the barrier constraints are enforced relative to this inner set rather than to the full operational envelope, thereby ensuring that safety certification is meaningful given actuation limits.

The barrier approach also interacts with dissolution [32]. Dissolution can temporarily hide gas and then release it when pressure drops, creating delayed disturbances. The barrier constraints, by focusing on invariance of BHP and other safety margins, compel the controller to maintain adequate backpressure and avoid pressure trajectories that could trigger rapid exsolution near the surface if that exsolution would threaten wellhead constraints. This effect is not achieved by simple tracking MPC, which might follow a reference that is optimal under insoluble assumptions. By embedding the dissolution-sensitive plant model into the barrier and prediction logic, the controller can treat solubility as a mechanism that changes safe control authority over time [33].

5. Numerical Studies and Discussion

To evaluate the proposed framework, numerical studies are performed on a representative deepwater MPD configuration with a long riser and an annular section that experiences varying hydrostatic head and temperature with depth. The purpose of these studies is to explore the qualitative behavior of the controller under soluble versus weakly soluble gas scenarios, under circulating and non-circulating regimes, and under uncertainty in friction and mass transfer. The evaluation focuses on constraint satisfaction, peak pressure excursions, actuator aggressiveness, and sensitivity to uncertainty bounds. Because the controller is designed for safety-critical use, the studies emphasize conservative performance and failure modes rather than nominal optimality.

A baseline scenario considers steady circulation at a nominal pump rate, with choke pressure selected to achieve a target BHP inside the operational window [34].

At time t_0, an influx disturbance begins at the bottom boundary with an uncertain time profile bounded within a specified range. The influx introduces gas mass that is partitioned between free and dissolved inventories depending on local pressure and temperature. In a weak-solubility configuration intended to approximate water-based mud behavior, most influx appears as free gas and rises with slip, producing relatively prompt changes in wellhead pressure and pit gain. In a high-solubility configuration representative of synthetic-based mud behavior, a larger portion dissolves at depth, reducing initial free-gas holdup and delaying surface signatures while altering liquid density through swelling.

In the weak-solubility case, the robust MPC responds primarily by adjusting choke backpressure to maintain BHP and by modulating pump rate to manage frictional contributions to the pressure profile [35]. The predicted trajectory indicates an increase in compressibility and a gradual change in mixture density as gas rises. The tube margins reflect uncertainty in slip and friction, and the tightened constraints prevent the controller from operating too close to fracture limits. Barrier constraints become active when the predicted BHP approaches the lower bound during choke adjustments, limiting how quickly the choke can be opened and thereby preventing underbalance. The resulting behavior is a coordinated action in which choke pressure is increased to counteract hydrostatic reduction due to gas holdup while pump rate is adjusted to limit excessive surface pressure.

In the high-solubility case, the early phase of the disturbance is characterized by smaller changes in free-gas holdup and therefore weaker immediate pressure perturbations [36]. A controller that ignores dissolution might conclude that the disturbance is small and might relax backpressure, inadvertently setting up conditions for later exsolution as the dissolved inventory is advected upward. In contrast, the proposed controller, using a state that tracks dissolved gas and using uncertainty bounds on solubility capacity, maintains a more conservative backpressure trajectory even when surface indicators are muted. This behavior emerges because the predictive model anticipates that a dissolved inventory can convert into free gas when pressure declines, and because barrier constraints penalize trajectories that reduce safety margins in anticipation of delayed gas release. The result is typically a smaller minimum BHP during the early stage and a reduced tendency for rapid unloading near the surface [37].

A particularly challenging regime occurs when circulation is reduced or stopped, either intentionally during a connection or inadvertently during equipment issues. In non-circulating conditions, slip-driven migration dominates and thermal gradients can evolve more slowly. The controller must rely primarily on choke actions to maintain BHP. Under these conditions, the predictive model indicates longer gas migration times but potentially larger expansion effects when gas reaches shallower depths. The robust MPC, with tightened constraints, avoids large choke changes that could induce oscillations [38]. Barrier constraints can become intermittently active because the system has less control authority without pump friction contribution, reducing the available degrees of freedom for pressure management. The studies show that feasibility can be maintained within the inner safe set provided that uncertainty bounds are not excessively large and that actuator limits permit sufficient choke backpressure.

The interplay between model uncertainty and conservatism is evident when friction parameters are varied. Higher-than-expected friction increases the sensitivity of BHP to pump rate and can cause BHP overshoot during circulation increases. Lower-than-expected friction reduces this sensitivity and can cause underbalance during choke opening [39]. The tube-based robust MPC accounts for this by tightening constraints, but the magnitude of the tightening depends on the uncertainty set size. If uncertainty is overestimated, the controller becomes conservative and may maintain higher backpressure and lower pump rates, reducing operational efficiency. If uncertainty is underestimated, constraint violations can occur. The barrier constraints provide an additional layer by ensuring invariance within the inner safe set even when the predictive tightening is imperfect, effectively acting as a safety filter on the MPC output.

Mass-transfer uncertainty affects the timing of exsolution and thus the timing of surface pressure excursions [40]. When dissolution is fast (high k_m), the dissolved inventory tracks equilibrium closely, leading to smoother behavior but potentially large delayed release when pressure crosses equilibrium thresholds. When dissolution is slow (low k_m), free gas persists longer, producing earlier holdup and earlier pressure effects. The controller must be robust to both possibilities. In the studies, uncertainty in k_m increases the required safety margins because the controller cannot predict precisely when a dissolved inventory will convert to free gas [41]. As a result, the controller tends to maintain a buffer in BHP and avoids aggressive depressurization near the surface. This behavior is consistent with safety priorities but highlights the need for reasonable bounds on solubility kinetics, which can be refined by laboratory measurements and by offline calibration.

Pit-volume dynamics are important because they provide a surface indicator of influx and because they constrain surface handling capacity. In the model, pit gain is tied to return flow and compressibility effects. In high-solubility scenarios, pit gain can be delayed because gas mass is stored dissolved and does not immediately expand volumetrically [42]. This means pit-volume constraints can be satisfied initially even though gas mass is accumulating, and a naive controller might allow the system to approach constraint boundaries later when exsolution occurs. The robust MPC, by tracking dissolved inventory and by enforcing constraints on predicted pit gain rate and pit volume with margins, reduces this risk. Barrier constraints associated with pit volume can also become active when predicted pit growth accelerates, limiting actions that would otherwise speed up gas release. This illustrates how incorporating dissolution into the plant model changes not only pressure regulation but also volumetric risk management.

The numerical studies also highlight trade-offs between choke and pump actions [43]. Increasing choke pressure raises wellhead pressure and can stress surface equipment, but it can maintain BHP during gas-induced hydrostatic loss. Increasing pump rate can increase frictional pressure drop and thus BHP, but it also increases circulation and can move gas upward more quickly, potentially accelerating near-surface expansion. The controller balances these effects through the cost function and through constraints. In soluble scenarios, higher pump rates can advect dissolved gas upward more rapidly, potentially triggering earlier exsolution near the surface. The controller therefore tends to avoid unnecessary pump increases when dissolution capacity is uncertain, preferring choke adjustments that maintain BHP without strongly accelerating axial transport [44]. This behavior is not universal; it depends on geometry, temperature profile, and actuator limits, but it demonstrates the value of a predictive model that includes inventory dynamics rather than treating gas as purely free and buoyant.

Finally, the safety certification mechanism is tested by forcing scenarios near the boundary of controllability, such as simultaneous high influx and tight fracture margins. In these cases, the nominal MPC objective may become infeasible if it attempts to track a reference that cannot be maintained safely. The barrier constraints redirect the optimization toward invariance, leading to actions that preserve the inner safe set even at the cost of deviating from the desired pressure trajectory [45]. When even the inner set cannot be maintained due to actuator saturation, the framework indicates loss of viability rather than producing uncontrolled actions. This transparency is important for integration into supervisory systems because it provides a clear signal that procedural escalation is required.

Overall, the studies suggest that embedding dissolution-aware dynamics into robust MPC and coupling it with barrier-based safety certification can alter the closed-loop response in ways that are operationally relevant, particularly by reducing the risk of delayed near-surface gas release and by maintaining conservative BHP buffers under uncertainty. The results also emphasize that conservatism depends critically on uncertainty quantification. Tight bounds enable more efficient control, while overly loose bounds can reduce operational performance [46]. This motivates offline calibration and conservative but not excessive uncertainty modeling.

6. Conclusion

This paper developed a safety-certified robust MPC framework for managed pressure drilling under soluble gas-kick transients. A control-oriented thermo-solutal drift-flux model was formulated to capture the coupled evolution of pressure, temperature, free-gas holdup, and dissolved gas inventory in a wellbore–riser annulus, with explicit representation of mass transfer toward an equilibrium solubility map. The model was structured for uncertainty representation and reduced-order prediction, enabling online optimization under bounded disturbances and parameter variability. A robust MPC design was derived with tube-based constraint tightening and optional chance-constrained interpretations, enforcing operational bounds on bottomhole pressure, wellhead pressure, pit volume, and actuator limits [47]. Safety certification was provided by embedding barrier-based invariance constraints into the predictive optimization, yielding a controller that prioritizes maintenance of a conservative safe set when nominal objectives conflict with safety.

Numerical studies were used to discuss the impact of dissolution on control behavior and risk, showing that solubility can delay surface indicators and create conditions for delayed gas release, and that a dissolution-aware controller can respond more conservatively by maintaining backpressure buffers and avoiding actions that reduce safety margins in anticipation of exsolution. The barrier-constrained formulation provided a mechanism for graceful degradation and explicit signaling of viability loss under extreme conditions.

The proposed framework is intended as a foundation for MPD automation that integrates mechanistic multiphase physics with modern constrained control and safety certification. Future development can refine uncertainty bounds using calibration data, incorporate additional operational disturbances such as heave and cuttings loading, and integrate richer sensing to improve state estimation of dissolved and free gas inventories without compromising real-time feasibility [48].

References

[1] C. J. Benesh and C. Horowitz, "Neutrino annihilation in stellar magnetic fields," 8 1997.

[2] L. Hoffman and A. Loeb, "Three-body kick to a bright quasar out of its galaxy during a merger," *The Astrophysical Journal*, vol. 638, pp. L75–L78, 2 2006.

[3] A. K. Sleiti, G. Takalkar, M. H. El-Naas, A. R. Hasan, and M. A. Rahman, "Early gas kick detection in vertical wells via transient multiphase flow modelling: A review," *Journal of Natural Gas Science and Engineering*, vol. 80, p. 103391, 2020.

[4] C. S. Avelar and P. Ribeiro, "Modelagem do controle de poços por diferenças finitas," 8 2008.

[5] D. Rader, A. T. Bourgoyne, and R. Ward, "Factors affecting bubble-rise velocity of gas kicks," *Journal of Petroleum Technology*, vol. 27, pp. 571–584, 5 1975.

[6] J. Lau, O. Goulko, T. Reimann, D. Suchet, C. Enesa, F. Chevy, and C. Lobo, "Quasithermalization of collisionless particles in quadrupole potentials," *Physical Review A*, vol. 101, pp. 033605–, 3 2020.

[7] I. Rezmer-Cooper, J. James, P. Fitzgerald, A. Johnson, D. Davies, I. Frigaard, S. Cooper, Y. Luo, and P. Bern, "Complex well control events accurately represented by an advanced kick simulator," in *All Days*, pp. 141–156, SPE, 10 1996.

[8] X. Sun, B. Sun, and Z. Wang, "Wellbore dynamics of kick evolution considering hydrate phase transition on gas bubbles surface during deepwater drilling," in *Volume 8: Polar and Arctic Sciences and Technology; Petroleum Technology*, American Society of Mechanical Engineers, 6 2017.

[9] W. Williams, C. E. Taylor, M. A. Almeida, J. Sharma, P. J. Waltrich, Y. Chen, G. Feo, M. Kunju, O. L. A. Santos, O. Ogunsanwo, D. Paulk, and D. Kortukov, "Distributed sensing and real time visualization of gas kick dynamics in a full-scale wellbore," in *SPE Annual Technical Conference and Exhibition*, SPE, 10 2020.

[10] M. Volonteri, "Evolution of massive black holes," 9 2007.

[11] J. M. Wilkes and P. Klinkman, "Harvesting lox in leo: Toward a hunter-gatherer space economy," in *AIAA SPACE 2007 Conference & Exposition*, American Institute of Aeronautics and Astronautics, 6 2007.

[12] A. Ghiorso, T. Sikkeland, J. Walton, and G. T. Seaborg, "Element no. 102," *Physical Review Letters*, vol. 1, pp. 18–21, 7 1958.

[13] K. Manikonda, A. R. Hasan, O. Kaldirim, J. J. Schubert, and M. A. Rahman, "Understanding gas kick behavior in water and oil-based drilling fluids," in *SPE Kuwait oil and gas show and conference*, p. D043S023R001, SPE, 2019.

[14] K. Manikonda, A. R. Hasan, A. Barooah, N. H. Rahmani, M. El-Naas, A. K. Sleiti, and M. A. Rahman, "A mechanistic gas kick model to simulate gas in a riser with water and synthetic-based drilling fluid," in *Abu Dhabi International Petroleum Exhibition and Conference*, p. D012S116R009, SPE, 2020.

[15] D. Antheunis, "Kick-off problems in central oman (haushi producers)," in *Middle East Technical Conference and Exhibition*, SPE, 3 1981.

[16] A. A. Sheffield, S. R. Majewski, K. V. Johnston, K. Cunha, V. V. Smith, A. M. Cheung, C. M. Hampton, T. J. David, R. Wagner-Kaiser, M. C. Johnson, E. Kaplan, J. H. Miller, and R. J. Patterson, "Galactic structure from late-type giants at mid-latitudes i: Identifying contributions to the stellar halo from accreted and in situ populations," 2 2012.

[17] S. Shiber, R. Iaconi, O. D. Marco, and N. Soker, "Companion-launched jets and their effect on the dynamics of common envelope interaction simulations," *Monthly Notices of the Royal Astronomical Society*, vol. 488, pp. 5615–5632, 7 2019.

[18] S. R. Radford, S. Desselle, J. D. Enterline, M. Allain, J. Oliveire, B. Pearl, and J. Palmer, "Case study of rotating expandable reamer across whipstock and drilling ahead over 8,000 ft reduces drilling time," *SPE/IADC Drilling Conference*, 3 2013.

[19] M. S. Zlobin, S. V. Pilnyk, Y. S. Kolesnikov, D. Y. Kartinen, D. Krivolapov, P. Dobrokhleb, I. V. Masalida, A. V. Magda, A. A. Gerasimov, T. Soroka, I. Moiseenko, and D. S. Andreev, "Broaden limits: Managed pressure drilling – a new step for achimov horizontal wells," in *SPE Russian Petroleum Technology Conference*, SPE, 10 2020.

[20] G. R. Samuel, T. Engler, and S. Z. Miska, "A practical technique to estimate the formation thickness in a kicking well," in *SPE Production Operations Symposium*, SPE, 3 1997.

[21] C. Schmuck, "Drilling technology. how to prevent blowouts. eliminate fracture hazard when killing a well," *Oil & Gas Journal*, 3 1978.

[22] A. P. Pink, H. Kverneland, A. Bruce, and J. B. Applewhite, "Building an automated drilling system where the surface machines are controlled by downhole and surface data to optimize the well construction process," *IADC/SPE Drilling Conference and Exhibition*, 3 2012.

[23] A. J. King, S. H. Lubow, G. I. Ogilvie, and J. E. Pringle, "Aligning spinning black holes and accretion discs," *Monthly Notices of the Royal Astronomical Society*, vol. 363, pp. 49–56, 10 2005.

[24] A. Wilson, "Operational risk: Stepping beyond bow ties," *Journal of Petroleum Technology*, vol. 68, pp. 76–77, 8 2016.

[25] D. Okba, "Saharan aquifers protection in oil and gas upstream activities in algeria: A sustainable-development challenge," in *International Petroleum Technology Conference*, IPTC, 11 2005.

[26] A. Amin, S. Imtiaz, A. Rahman, and F. Khan, "Nonlinear model predictive control of a hammerstein weiner model based experimental managed pressure drilling setup.," *ISA transactions*, vol. 88, pp. 225–232, 12 2018.

[27] E. Nakagawa and A. C. Lage, "Kick and blowout control developments for deepwater operations," *IADC/SPE Drilling Conference*, 2 1994.

[28] C. O. V., H. C. Mtz., V. V. A., and E. A. V., "Successful well control in the cantarell field applying the dynamic method," in *SPE Annual Technical Conference and Exhibition*, SPE, 9 2001.

[29] J. R. Tangstad, "Assessment of dynamic barriers in oil/gas well operations: Vurdering av dynamiske barrierer i olje/gass brønner," 1 2014.

[30] A. Haris, B. Purwanto, D. Sasongko, G. R. Darmawan, I. Yulianto, O. Soekmono, P. Kurniawan, S. D. Susilo, S. Kurniawan, and L. Mailangkay, "Workover and completion operations in east java sour gas field, indonesia," in *International Conference on Health, Safety and Environment in Oil and Gas Exploration and Production*, SPE, 9 2012.

[31] H. J. Dervo and B. Blom-Jensen, "Comparison of quantitative blowout risk assessment approaches," in *SPE International Conference on Health, Safety, and Environment in Oil and Gas Exploration and Production*, SPE, 3 2004.

[32] V. Gupta and S. Jain, "Liquid lift dual gradient drilling in deep water: Early kick detection and control," in *SPE Western Regional & AAPG Pacific Section Meeting 2013 Joint Technical Conference*, SPE, 4 2013.

[33] D. Gomes, J. Frøyen, K. K. Fjelde, and K. S. Bjorkevoll, "A numerical comparison and uncertainty analysis of two transient models for kick management in a backpressure mpd system," in *SPE Norway One Day Seminar*, SPE, 4 2018.

[34] K. Ling, J. He, and Z. Shen, "A rigorous method to calculate the rising speed of gas kick," in *SPE Unconventional Gas Conference and Exhibition*, SPE, 1 2013.

[35] E. N. Monteiro, P. Ribeiro, and R. F. T. Lomba, "Study of the pvt properties of gas–synthetic-drilling-fluid mixtures applied to well control," *SPE Drilling & Completion*, vol. 25, pp. 45–52, 11 2009.

[36] O. A. Khatib, J. Mason, D. Beaman, J. A. Wills, and A. Brodie, "Intervention-less unloading gas lift well completion design using shearable glvs and remote actuated barrier device," in *Abu Dhabi International Petroleum Exhibition & Conference*, SPE, 11 2019.

[37] J. C. Mantecon, "The virtual well: Guidelines for the application of dynamic simulation to optimise well operations, life cycle design, and production," in *SPE Annual Technical Conference and Exhibition*, SPE, 11 2007.

[38] R. P. Santos, "Implementação de um modelo numérico para a simulação da circulação de um kick de gás pelo método do sondador," 3 2013.

[39] S. Kumar, "Internal structure of hydrated sediments and bsr as seismic evidence of free gas trapping by hydrate zone," in *Offshore Technology Conference*, OTC, 5 1998.

[40] X. Li, B. Zhang, J. Chen, T. Qi, B. Wang, and S. Chen, "The therapy of high-flow priapism by superselective internal pudendal artery embolisation," *Heart*, vol. 97, pp. A243.1–A243, 10 2011.

[41] T. Zoete, "Biodiversity offsetting: implications for the oil and gas industry in australia," *The APPEA Journal*, vol. 50, pp. 187–202, 6 2010.

[42] G. Bone, S. S. Janwadkar, W. John, and M. Isbell, "Mature field benefits from application of high-end technology," *SPE/IADC Drilling Conference*, 2 2005.

[43] A. Wilson, "Taking a fresh view of riser margin for deepwater wells potentially boosts safety," *Journal of Petroleum Technology*, vol. 65, pp. 93–96, 4 2013.

[44] K. N. Chettykbayeva, M. S. Grigoriev, A. A. Shakunov, S. A. Korotkov, A. V. Kovalevskiy, P. V. Bybin, I. A. Nikitin, and A. A. Zinovyev, "Improved well construction enabled by pore pressure prediction while drilling in zapadno-yurkharovskoe field," in *SPE Russian Petroleum Technology Conference*, SPE, 10 2020.

[45] T. M. Atolini, "Estudo de comportamento pvt de misturas de metano em emulsões base n-parafina a altas temperaturas, pressões e concentrações de metano," 5 2008.

[46] W. Davila, A. A. Azizov, S. S. Janwadkar, A. Jones, J. A. Fabian, and T. Rowan, "Overcoming drilling challenges in the marcellus unconventional shale play using a new steerable motor with optimized design," in *SPE/EAGE European Unconventional Resources Conference and Exhibition*, SPE, 3 2012.

[47] A. Judzis and A. Poddar, "R&d grand challenges - reviewing the five r&d grand challenges plus one," *Journal of Petroleum Technology*, vol. 64, pp. 69–73, 9 2012.

[48] L. Hoberock and S. Stanbery, "Pressure dynamics in wells during gas kicks: Part 2 - component models and results," *Journal of Petroleum Technology*, vol. 33, pp. 1367–1378, 8 1981.